HYDRA2

A Multispectral Data Analysis Toolkit for Sensors on *Suomi-NPP* and Other Current Satellite Platforms

BY TOM RINK, W. PAUL MENZEL, LIAM GUMLEY, AND KATHY STRABALA

A freeware application for remote sensing, multispectral/hyperspectral data analysis, and interrogation with *Suomi-NPP*, NASA's *Terra* and *Aqua*, EUMETSAT's MetOp, and the Chinese's *Fengyun-3* satellites.

The Hyperspectral Data Viewer for Development of Research Applications, version 2 (HYDRA2), is an update to the capabilities of HYDRA (Rink et al. 2007). The "HYDRA" concept is based on over 10 years of continued development of interactive satellite data interrogation and visualization tools offered at the University of Wisconsin–Madison's (UW) Space Science and Engineering Center's (SSEC) remote sensing workshop series (http://cimss.ssec.wisc.edu/rss/) and direct broadcast seminars (http://cimss.ssec.wisc.edu/dbs/). The salient requirements for HYDRA2 remain similar to those of its predecessor: it must be 1) freely available to the global community, 2) computer platform independent, and 3) extendable. Essentially, HYDRA2 is a stand-alone application based on the Visualization for Algorithm Development (VisAD; Hibbard et al. 2002) Java library to integrate data from various satellite sensors, ground-based instruments, and forecast models into very interactive and high-performance 2D/3D displays.

A primary motivation of this new effort is to support the *Suomi–National Polar-Orbiting Partnership* (*Suomi-NPP*) and the upcoming Joint Polar Satellite System (JPSS) missions, as well as maintaining existing support for the Moderate Resolution Imaging Spectroradiometer (MODIS) sensors on board the *Terra* and *Aqua* platforms. To achieve this, HYDRA2's custom VisAD data adapters for cross-track polar swath were improved to have greater flexibility and a more clearly defined programmatic interface. These improvements also facilitated the transitioning of datasets on board the Meteorological Operation (MetOp) and Fengyun (FY) satellite series into HYDRA2 with only a modest level of effort.

HYDRA2 enables the user to inspect multispectral (broadband and hyperspectral) fields of data so that 1) spectral measurements can be easily displayed at pixel locations; 2) colors can be assigned to pixel values and false color images can be viewed; 3) images of spectral band combinations can be constructed; 4) scatterplots can be determined from imagery

AFFILIATIONS: RINK, MENZEL, GUMLEY, AND STRABALA—Space Science and Engineering Center, University of Wisconsin–Madison, Madison, Wisconsin
CORRESPONDING AUTHOR: W. Paul Menzel, Space Science and Engineering Center, University of Wisconsin–Madison, 1225 West Dayton Street, Madison, WI 53706
E-mail: paul.menzel@ssec.wisc.edu

The abstract for this article can be found in this issue, following the table of contents.

DOI:10.1175/BAMS-D-14-00285.1

In final form 11 September 2015

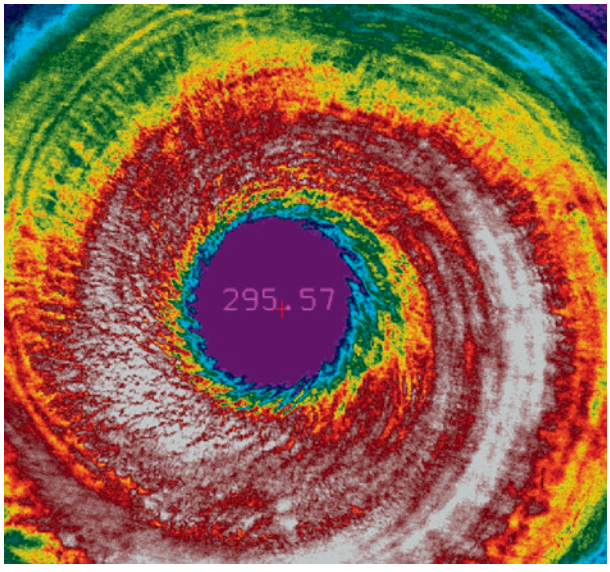

Fig. 1. VIIRS infrared window image (I5, 11.5 μm) of the eye of Typhoon Vongfong on 7 Oct 2014 with inverse rainbow color enhancement (reds start at 190 K, greens at 195 K, and blues end at 205 K). The brightness temperature in the eye of Typhoon Vongfong is 295.6 K.

containing individual or combined spectral bands, and individual pixel values can be obtained either from scatterplots or imagery; 5) transects of measurements from imagery can be displayed, and 6) measured spectra and the derived temperature and moisture profiles from individual pixels can be displayed and studied.

Many improvements in the user interface and analysis tools have been implemented in HYDRA2 based on ongoing user feedback. These include the following: 1) linking the zooming, roaming, and interrogating between multiple image display windows; 2) combining spectral bands or linear combinations of spectral bands from multiple sensors [e.g., MODIS and Visible Infrared Imaging Radiometer Suite (VIIRS)] onto a single image display; 3) managing datasets in a consistent manner; 4) eliminating VIIRS and MODIS cross-track scan "bowtie" artifacts in the regridding process; 5) aggregating consecutive and separate file granules into a single cohesive image; and 6) enabling image display export to Keyhole Markup Language (KML)/KML-zipped (KMZ) file formats for transport to Google Earth.

The evolution from HYDRA to HYDRA2 has been motivated, in part, by rapid advancements in software development technology over the last decade. HYDRA2 consists of a higher-functioning Java class–only application compared to the slower-performing Jython scripting language used in HYDRA. Perhaps more importantly, the software components that comprise HYDRA2 have been generalized so that any scripting language that supports Java (e.g., Jython or JRuby) can be used to develop, for example, a user-defined computation interface (Lutz 1996; Bill 2002). HYDRA2 employs the Java–netCDF library, which is the Java implementation of Unidata's Common Data Model (CDM), for access to Hierarchical Data Format release 4/5 (HDF4/5) format data, which are currently used in MODIS and several *Suomi-NPP* instruments. The Java–netCDF library merges the storage data models of many file formats—including, but not limited to, netCDF, versions 3 and 4 (netCDF3/4); Gridded Binary, editions 1 and 2 (GRIB1/2); and World Meteorological Organization (WMO) Binary Universal Form for Representation of Meteorological Data (BUFR)—to create a common application program interface (API) for many types of scientific data, including multidimensional arrays. This updated version effectively provides computer platform and storage format independent access from a single library.

HYDRA2 uses the NetBeans integrated development environment (IDE) from Oracle, which improves the processing efficiency of more robust source code development. HYDRA2 is deployed with platform-specific point-and-click installers generated by Install4j from EJ-Technologies. The YourKit Java profiler is employed to reduce any excessive and wasteful allocation of central processing unit (CPU) memory during runtime. Source code revision management is handled within a GitHub repository via Git integration in NetBeans. Unlike HYDRA, HYDRA2 is entirely self-contained within the installer; that is, no additional libraries are needed. Graphics card drivers still require upgrades, when necessary.

The following sections provide some examples of HYDRA2 analyzing data from *Suomi-NPP* that include VIIRS, the Cross-Track Infrared Sounder (CrIS), and the Advanced Technology Microwave Sounder (ATMS; see https://directory.eoportal.org/web/eoportal/satellite-missions/s/suomi-npp).

HYDRA2 is also capable of viewing and interrogating data from the *Terra* and *Aqua* platform sensors that include MODIS and the Atmospheric Infrared Sounder (AIRS; see https://directory.eoportal.org/web/eoportal/satellite-missions/a/aqua and https://directory.eoportal.org/web/eoportal/satellite-missions/t/terra). In addition, data from the MetOp (Klaes et al. 2007) Infrared Atmospheric Sounding Interferometer (IASI), the Advanced Very High Resolution Radiometer (AVHRR), the High

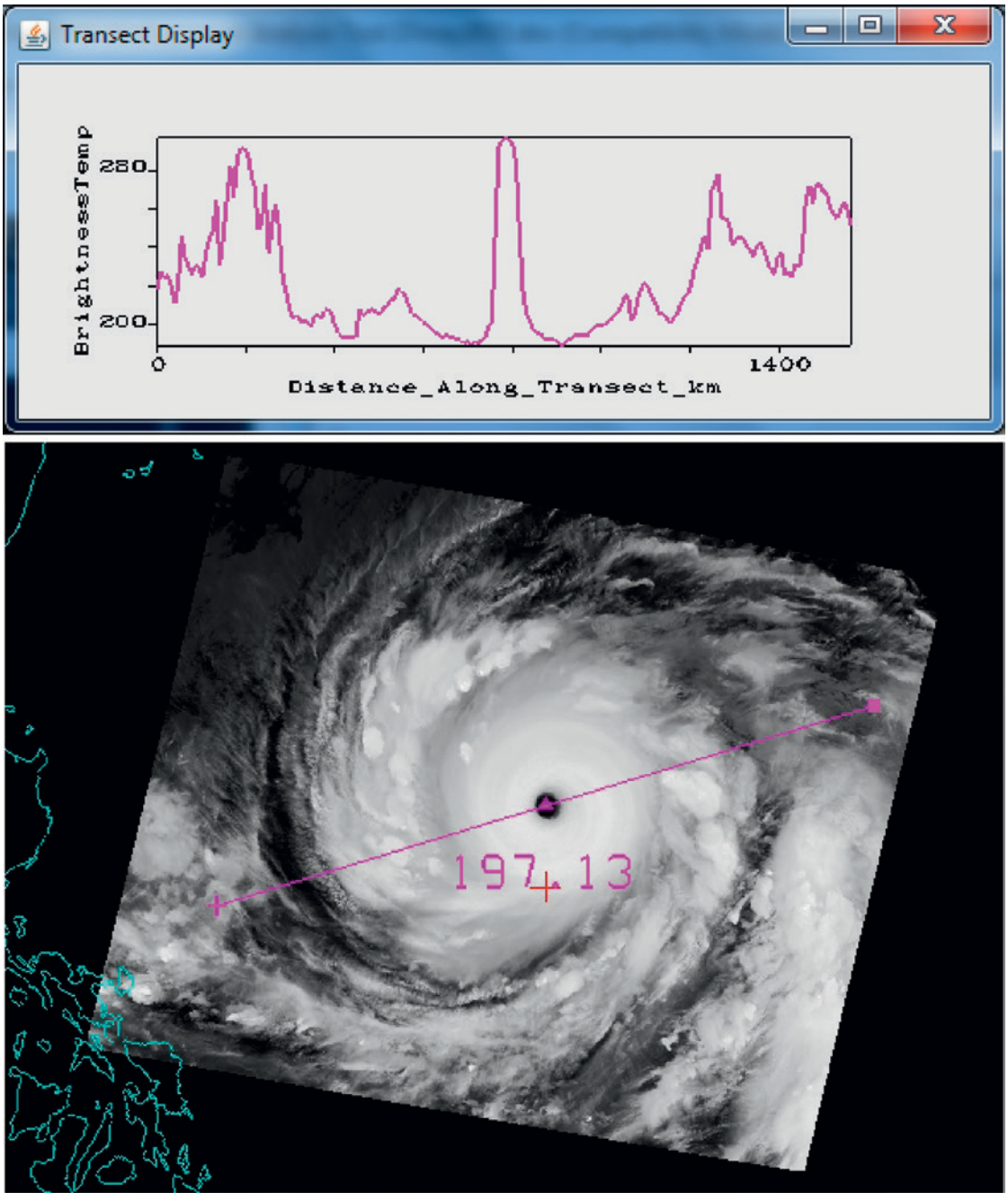

Fig. 2. (top) Infrared window brightness temperatures (K) for (bottom) the indicated transect in the 10.8-μm brightness temperature M15 image proceeding from left (west) to right (east). Distance along the transect is indicated (km).

Resolution Infrared Radiation Sounder (HIRS), and the Microwave Humidity Sounder (MHS) can also be displayed (see https://directory.eoportal.org/web/eoportal/satellite-missions/m/MetOp). And recently, data from the *FY-3* (see https://directory.eoportal.org/web/eoportal/satellite-missions/pag-filter/-/article/fy-3) Medium Resolution Spectral Imager (MERSI) were also added to the HYDRA2 capabilities.

EXAMPLES OF SPECTRAL BAND APPLICATIONS WITH HYDRA2. Expanding on the capabilities of HYDRA, HYDRA2 enables display and interrogation of the available spectral bands (22 for VIIRS and 36 for MODIS) for any pixel within a granule of data. Reflectance or brightness temperatures can be displayed for individual pixels within the granule. Red–green–blue (RGB) composites using any

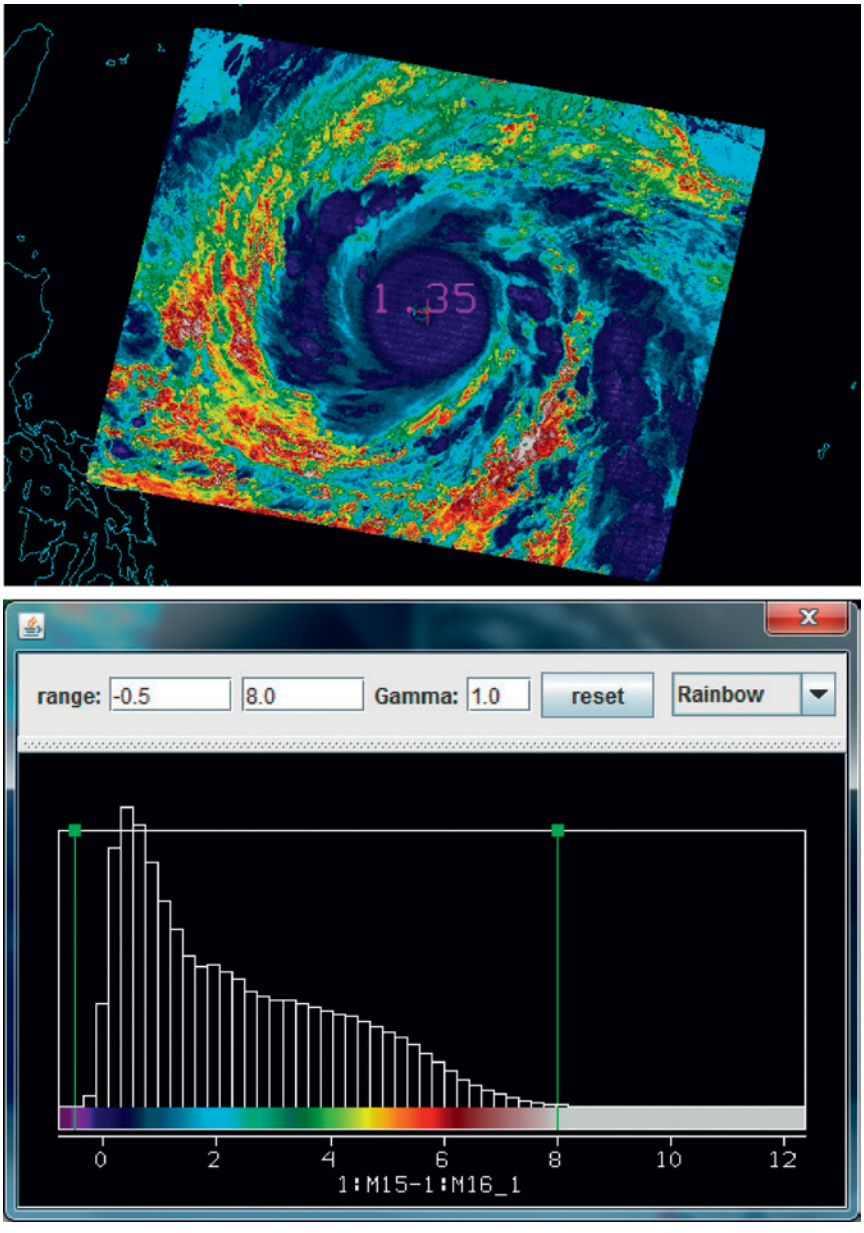

Fig. 3. (top) False color image of brightness temperature difference (K) between the water vapor–insensitive IR window (M15) and the water vapor–sensitive IR window (M16). (bottom) Color scale indicates the temperature difference along with histogram distribution within the image. Higher amounts of atmospheric moisture will produce larger differences; note the relative dryness above the high typhoon clouds.

combination of single and/or multispectral bands can be created. Transects from one location to another can be constructed for a given spectral band to determine a variety of remote sensing characteristics, for example, minimum/maximum values, pattern matching (clouds vs other features), and gradients.

Figure 1 shows the VIIRS infrared window I5 (11.45 μm) brightness temperature image of the eye of Typhoon Vongfong from 7 October 2012 in false color [with red (colder) and blue (warmer) in an inverse rainbow color enhancement]. The high spatial resolution (375 m) of VIIRS shows the eyewall structure in excellent detail. Using HYDRA2 commands, brightness temperature for each spectral band with corresponding locations (latitudes/longitudes) for each pixel can be displayed.

Figure 2 demonstrates the transect capability of HYDRA2. A transect is superimposed on the VIIRS infrared window M15 (10.8 μm) image, and the associated brightness temperature values are plotted from west to east along a 1500-km line centered on the eye of Typhoon Vongfong; brightness temperatures range from 190 K (cold, clouds near the eye) to 290 K (clear skies in the eye and farther away over warm ocean surfaces).

Differences of spectral bands are often useful in highlighting atmospheric or surface features. In Fig. 3, a VIIRS-derived split-window image was created using Band Math (IR window M15 at 10.8 μm minus the water vapor–sensitive IR window M16 at 12.0 μm); the brightness temperature difference is sensitive to atmospheric moisture, with larger differences usually indicating more moisture. The highest clouds associated with the typhoon on the southwest perimeter are readily apparent because of the dryness above the clouds (indicated by differences of less than 1 K).

The VIIRS day–night band (DNB, centered at 0.7 μm) is shown in Fig. 4 capturing the nighttime illumination over a segment of the Korean Peninsula at 1619 UTC 26 August 2012; the stark contrast between the brightly reflective industrialized regions covering

South Korea versus the unlit dark environment over North Korea is readily evident. In addition, fishing activity is also noticeable within the open water region to the east and southeast of South Korea. The DNB offers a new dimension of imaging capability, that of low-light visible reflectances at night. Miller et al. (2012) provide more details on the new remote sensing opportunities offered by the VIIRS DNB.

HYDRA2 has the capability to compare measurements between any two sensors. Figure 5 shows a comparison of the brightness temperatures measured by MODIS (band 31, 11.0 μm) in the bottom left and the VIIRS high-resolution imager (band I5, 11.5 μm) in the bottom right on 30 August 2012 over the southern portion of South Korea, the island of Jeju-do, and the open waters nearby. The overpass times are separated by less than 20 min. The higher spatial resolution of the VIIRS measurements (0.375 km) reveals sharper details than MODIS (1 km at nadir) across the coastline; this is evident in the annotated transect, where the corresponding brightness temperature plot reveals

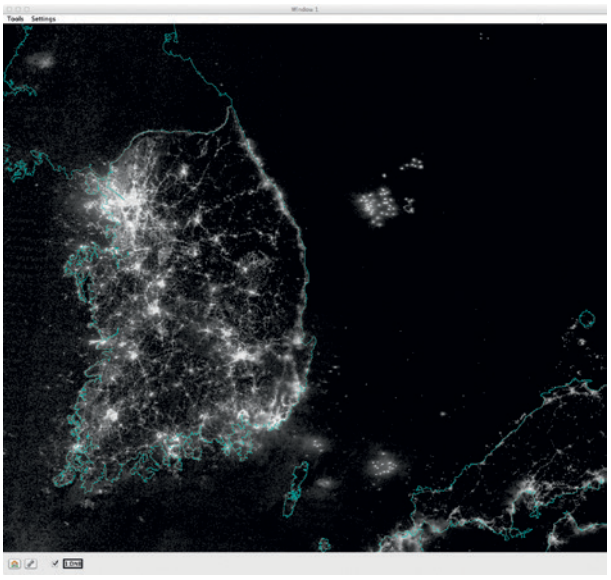

Fig. 4. VIIRS DNB image of the Korean Peninsula at 1619 UTC 26 Aug 2012. Lights from the cities and nighttime fishing are evident, as well as the stark contrast in lighting between North and South Korea.

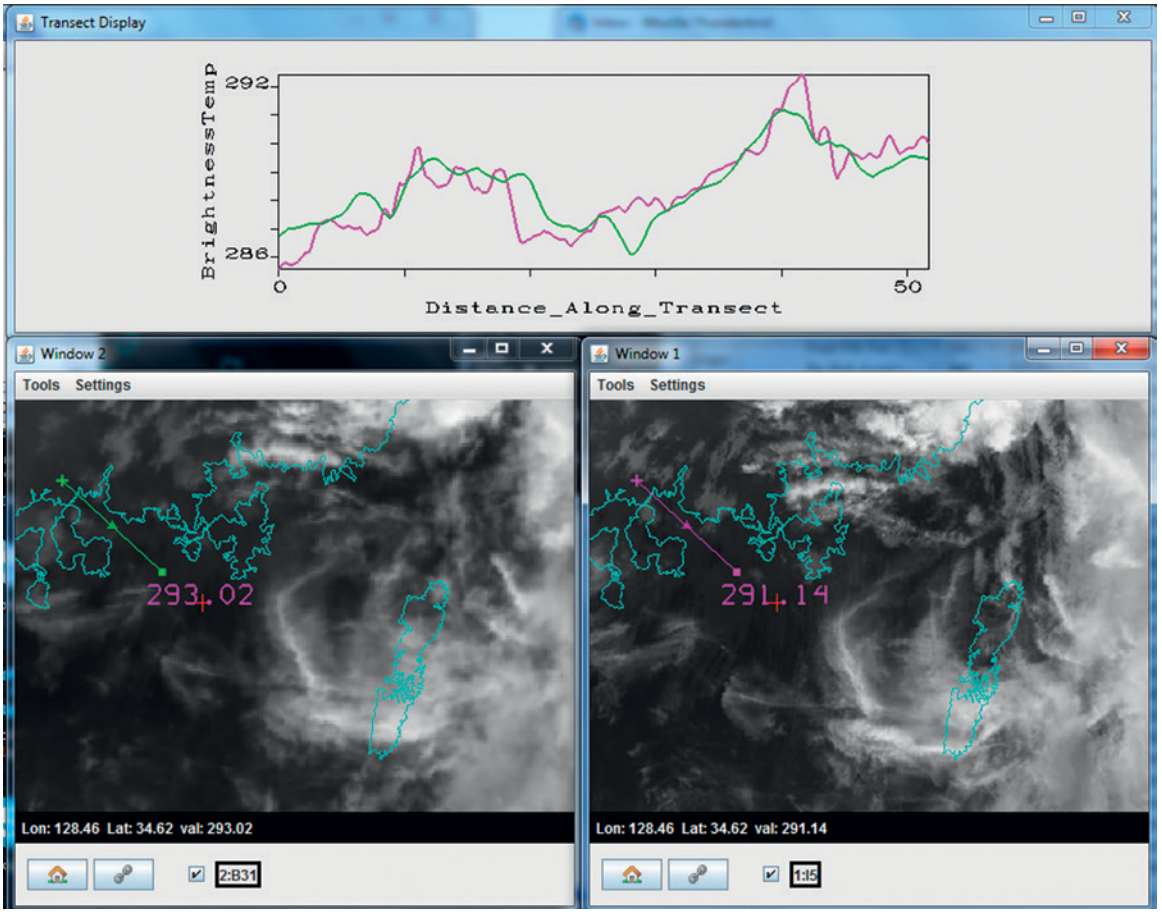

Fig. 5. Comparison of 30 Aug 2012 (bottom right) VIIRS 11.5-μm infrared window I5 at 375-m nadir resolution from 0422 UTC and (bottom left) corresponding MODIS 11.0-μm infrared window band 31 at 1-km nadir resolution from 0440 UTC, (top) along with a transect over clear skies. All units are in kelvins.

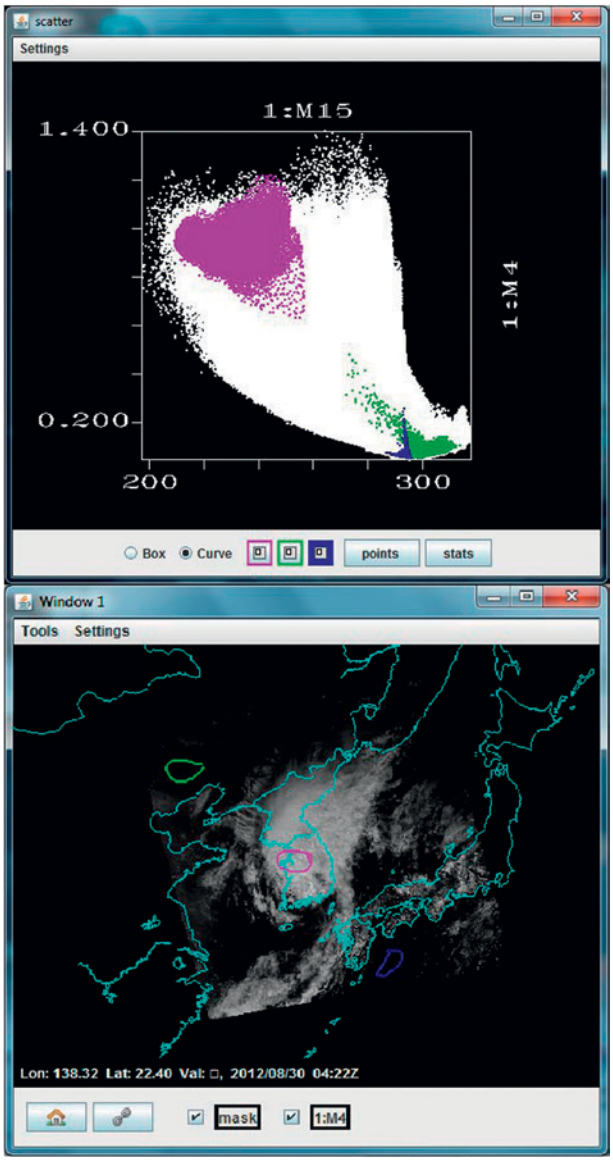

Fig. 6. (top) Scatterplot of visible band M4 0.55-μm reflectances (y axis) against infrared window band M15 10.8-μm brightness temperatures (x axis) at 0422 UTC 30 Aug 2012. Pixels in the scatterplot are highlighted in different colors and (bottom) their locations are marked in the visible 0.55-μm reflectance image. Purple highlights cold and reflecting cloud, green highlights warm and nonreflecting land, and blue highlights less-warm and nonreflecting ocean. The color mask can be clicked on and off with the check mark.

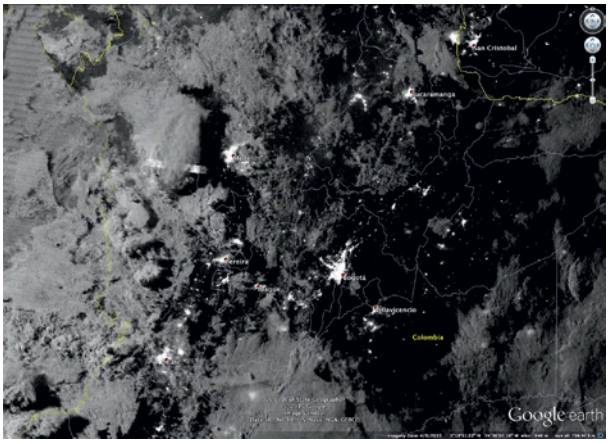

Fig. 7. An example of a nighttime VIIRS visible image on 30 Jan 2015 over Colombia as displayed over Google Earth, as part of HYDRA2 functionality.

a more detailed VIIRS profile (shown in magenta) versus the smoother MODIS profile (shown in green). The finer detail provided by VIIRS is most apparent away from nadir; VIIRS nadir resolution is constrained to grow by a factor of 2 across the entire swath, while the MODIS pixel size grows unconstrained to roughly 6 times by the edge of a narrower swath. In summary, HYDRA enables detailed comparisons of measurements between different sensors in transects, overlays, and scatterplots.

Figure 6 shows a scatterplot of visible (0.55 μm) reflectances plotted on the y axis against infrared window (10.8 μm) brightness temperatures on the x axis. Different colors highlight pixels in the scatterplot that are associated with regions circled in the visible reflectance image (purple shows cold and reflecting cloud pixels, green shows warm and nonreflecting vegetated surfaces, and blue shows warm and nonreflecting ocean). When two HYDRA windows have been established (containing a spectral band image, or spectral band combination image, or a derived product image), a scatterplot of the values in both windows can be compared against each other. In the scatterplot configuration, one can locate values either within the scatterplot or its corresponding imagery. Locating pixels in the scatterplot and associating them with pixels in the window display image—and vice versa—enables users to estimate threshold values for discriminating certain land, ocean, or atmospheric features.

Figure 7 shows the HYDRA2 display of the VIIRS DNB image over Colombia, South America, on 30 January 2015 transferred to Google Earth mapping; this enables the collocation tools from Google Earth to be applied to the HYDRA2 dataset. This example further demonstrates the ability to differentiate lightning versus city lights; west of the city lights around Medellin one finds illumination that cannot be associated with any city and is likely caused by cloud-to-cloud lightning.

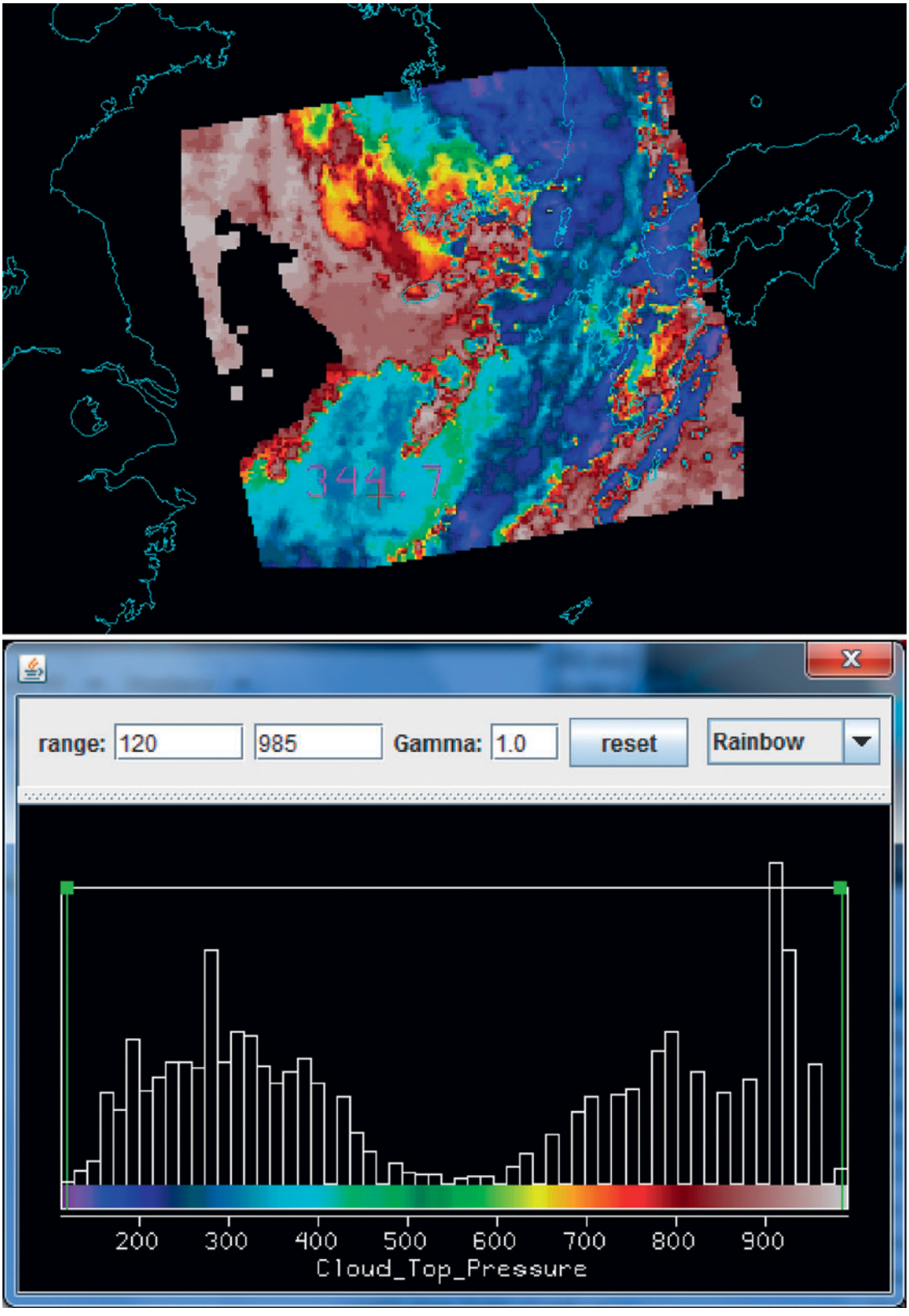

Fig. 8. (top) Derived image product of *Aqua* MODIS cloud-top pressure levels (hPa) from the MODIS level 2 (MOD06) cloud properties at 0440 UTC 30 Aug 2012. (bottom) Corresponding histogram and color code of cloud-top pressure levels within the entire image and associated color bar.

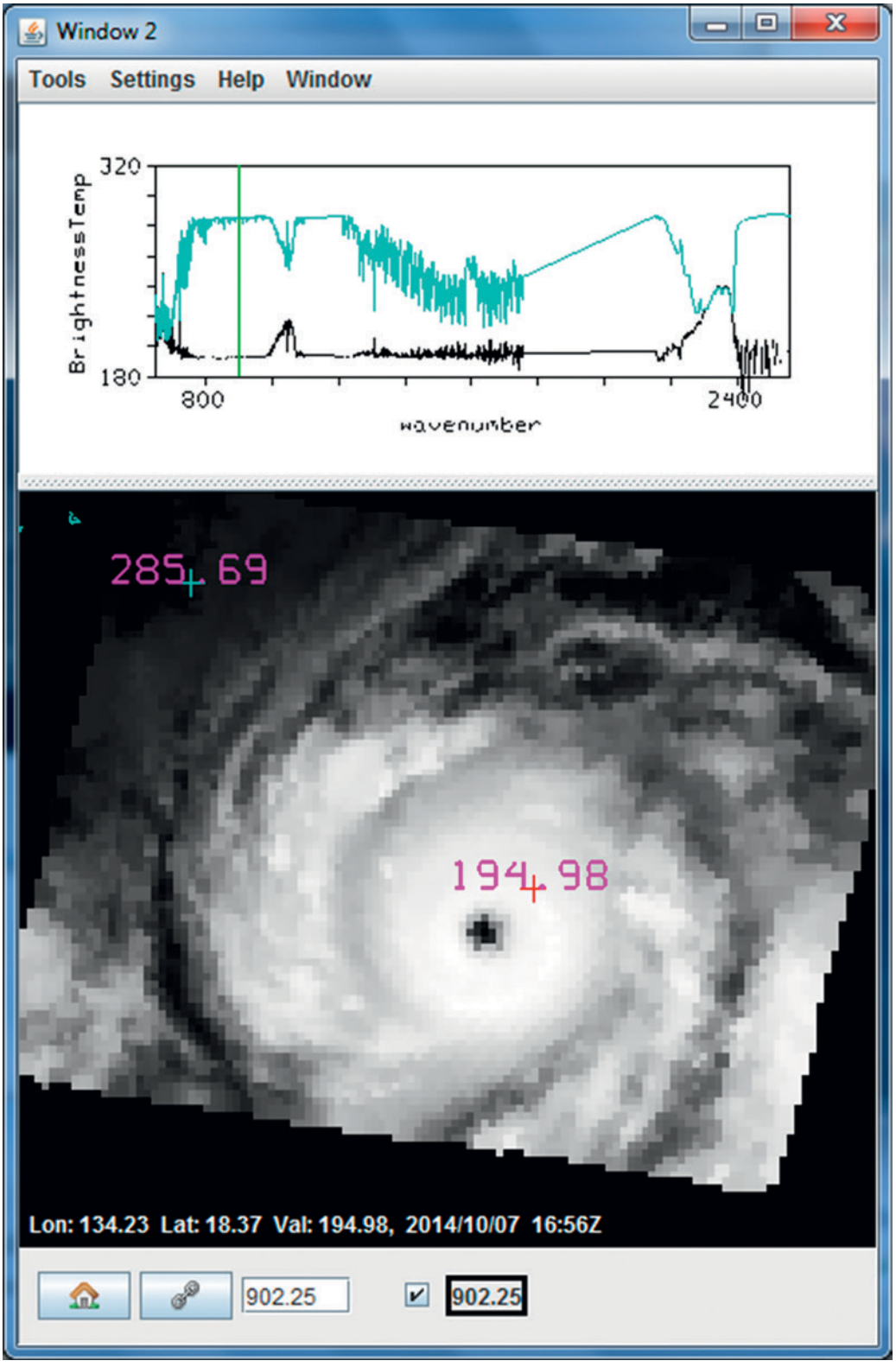

Fig. 9. (top) Black spectrum from clouds near the eye and turquoise spectrum from clear sky northwest of the typhoon. (bottom) Image of CrIS measurements [902 cm^{-1} brightness temperatures (K)] over Typhoon Vongfong on 7 Oct 2012 indicating the locations of the black spectrum (red cross) and the turquoise spectrum (turquoise cross).

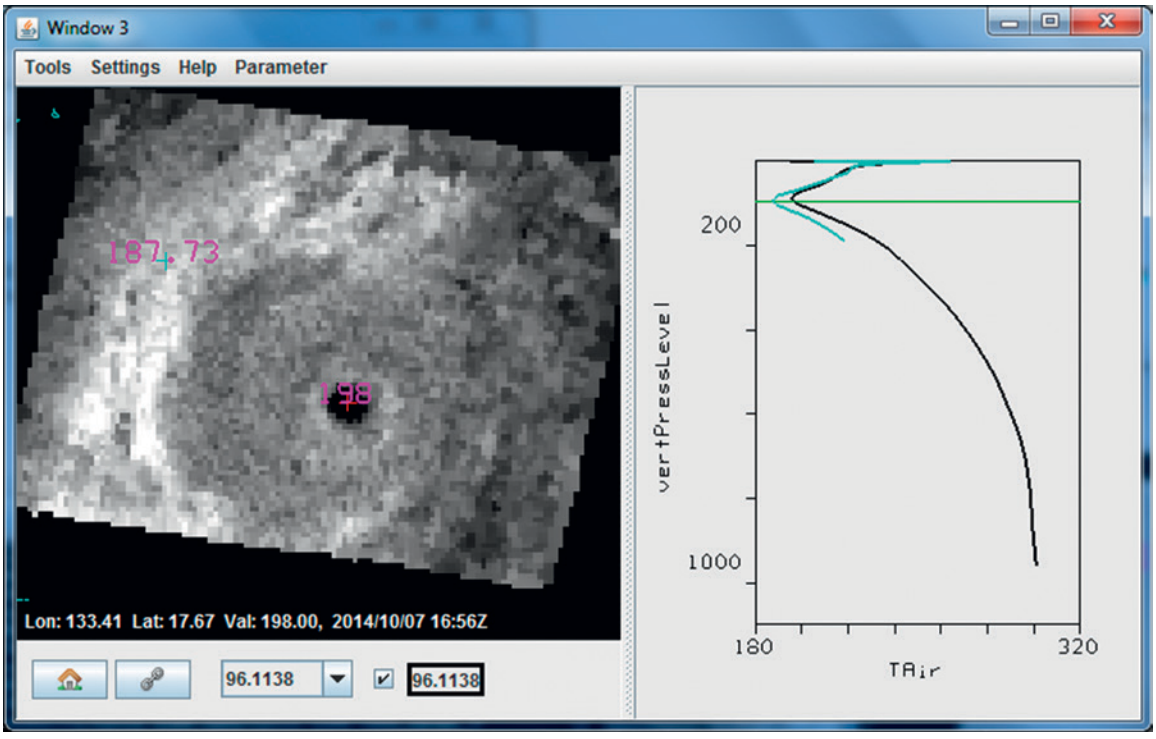

Fig. 10. (left) Display of temperatures at 96.1 hPa over Typhoon Vongfong on 7 Oct 2012 using the dual-regression retrieval, where white shades start at 185 K and black shades start at 195 K. (right) Temperature profile retrieval down to cloud top in the northwest sector of the typhoon (where the 96.1-hPa retrieved temperature is 187.73 K) is shown in black; the retrieval in the eye of the typhoon down to the ocean surface (where the 96.1-hPa temperature is 198.0 K) is shown in turquoise. The green line indicates the 96.1-hPa level.

HYDRA2 also has the capability to display several MODIS level 2 atmospheric product files, including the following:

MOD04: Aerosol products
MOD06: Cloud products (see Fig. 8 for an example display of the MODIS cloud-top pressure)
MOD14: Thermal anomalies—fires and biomass burning
MOD28: Sea surface temperature
MOD35: Cloud mask

Figure 8 shows the derived product image of the *Aqua* MODIS cloud-top pressure associated with 0440 UTC 30 August 2012; two cloud groups, the first at ~300 hPa and the second at ~800 hPa, are evident. HYDRA2 will incorporate the display of VIIRS environmental data record (EDR) products in the near future.

HYPERSPECTRAL AND MICROWAVE DATA ANALYSIS WITH HYDRA2. HYDRA2 can also be used to analyze granules of hyperspectral CrIS data in much the same way AIRS data were analyzed with HYDRA (Rink et al. 2007). Collocation in space and time is readily displayed with HYDRA2 for the VIIRS, CrIS, and ATMS sensors on *Suomi-NPP* (as well as with MODIS and AIRS sensors on *Terra* and *Aqua*, and the IASI sensors on MetOp). This section will demonstrate HYDRA2 analysis tools for viewing CrIS and ATMS data separately and together.

Figure 9 shows the HYDRA2 display of CrIS data over Typhoon Vongfong on 7 October 2012. The top panel displays a spectrum measured by CrIS over a clear pixel well away from the typhoon center (in turquoise) and another spectrum measured over clouds near the eye of the typhoon (in black). The brightness temperature infrared window image at 902.25 cm^{-1} (bottom panel) shows warm and cold regions. Within the spectrum plot, the clear brightness temperature spectrum (in black) shows the absorption of CO_2 at ~660 cm^{-1}, O_3 at ~1050 cm^{-1}, and H_2O at ~1500 cm^{-1} (causing notably cooler brightness temperatures in the positive lapse rate troposphere). The cloudy brightness temperature spectrum is remarkable for the near-constant temperature regardless of

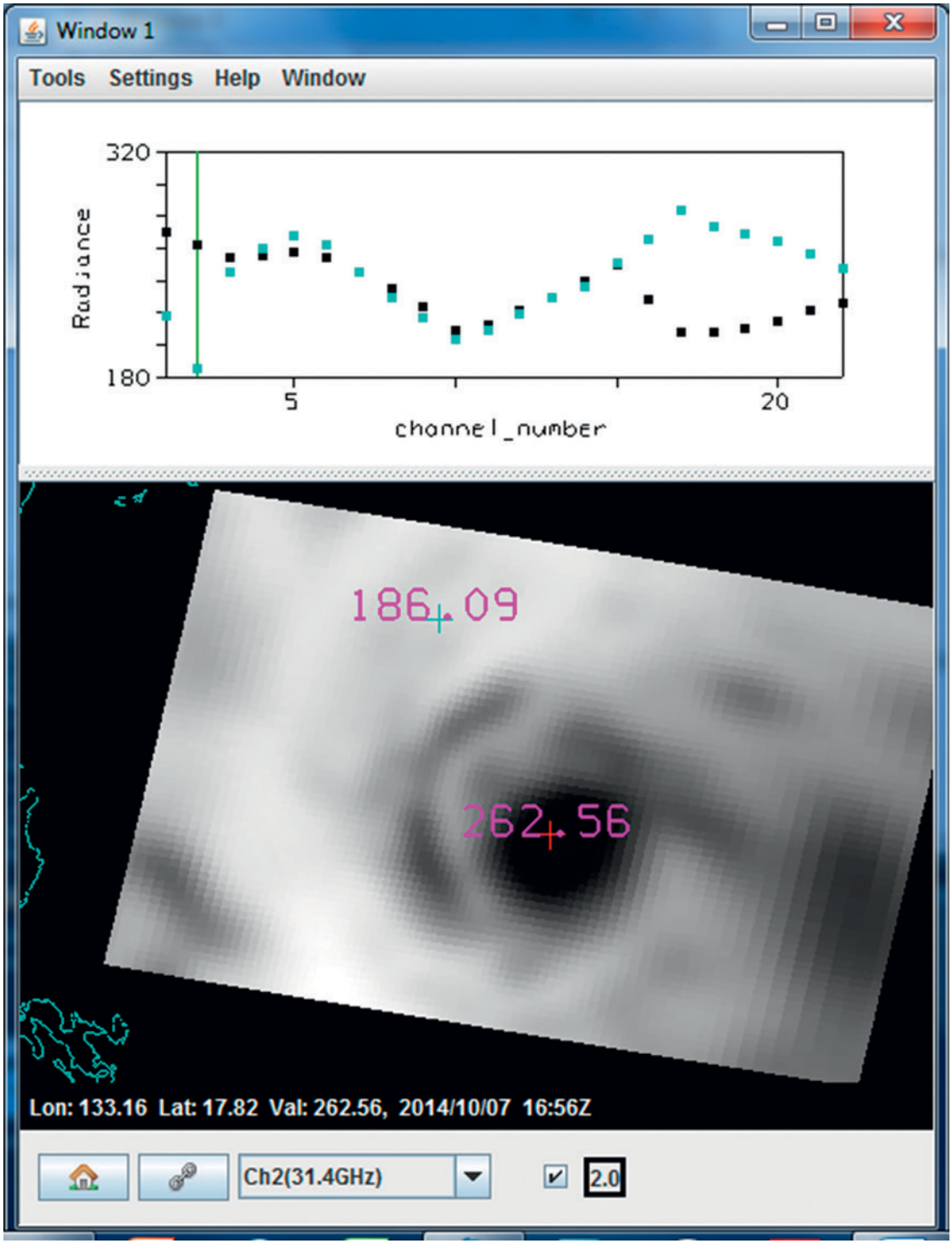

Fig. 11. (bottom) ATMS brightness temperature image for measurements over Typhoon Vongfong on 7 Oct 2012 at 31.4 GHz (channel 2), and (top) microwave spectra from channel 1 at 23 GHz to channel 22 at 183.3 GHz in clouds northwest of the typhoon center (turquoise dots) and in the eye (black dots).

wavenumber, indicating that the observed cloud is so high that above it there is very little H_2O and only small amounts of CO_2 and O_3 (causing somewhat warmer brightness temperatures in the negative lapse rate stratosphere).

CrIS measurements (at roughly 15-km spatial resolution) are used to derive temperature and moisture profiles in clear skies and above clouds (portions of the atmosphere where the measurements of at least some of the CrIS spectral bands are not

affected by clouds). Figure 10 shows the stratospheric temperatures at 96.1 hPa (above the typhoon) derived using a dual-regression profile retrieval (Weisz et al. 2013) along with a sounding of air temperature along the vertical pressure axis above the clouds at a position (annotated by 187.73 K) northwest of the typhoon and another position (annotated by 198 K) in the center of the eye. This remarkably well-formed eye, captured in a near-perfect nadir view by CrIS on *Suomi-NPP*, reveals warm temperatures (290–300 K) for the lowest 400 hPa in the troposphere.

ATMS measurements provide a sounding capability in clear and cloudy (nonprecipitating) conditions, albeit at relatively coarse (~50 km) spatial resolution. Figure 11 shows the image of ATMS brightness temperatures measured at 31.4 GHz (channel 2) over Typhoon Vongfong coincident with the VIIRS and CrIS data (shown in Fig. 10) along with brightness temperature spectra covering clear conditions (annotated by 262.56 K) within the eye and cloudy features (annotated by 186.09 K) to the northwest of the eye. The absorption features in the spectrum caused by O_2 (centered on channel 10 at 57.3 GHz) and H_2O (centered on channel 18 at 183.3 GHz) are evident as colder temperatures within the clear eye region. An additional contribution to the radiation in the microwave spectrum is the reflection from the surface (especially the ocean) in the more transparent spectral channels.

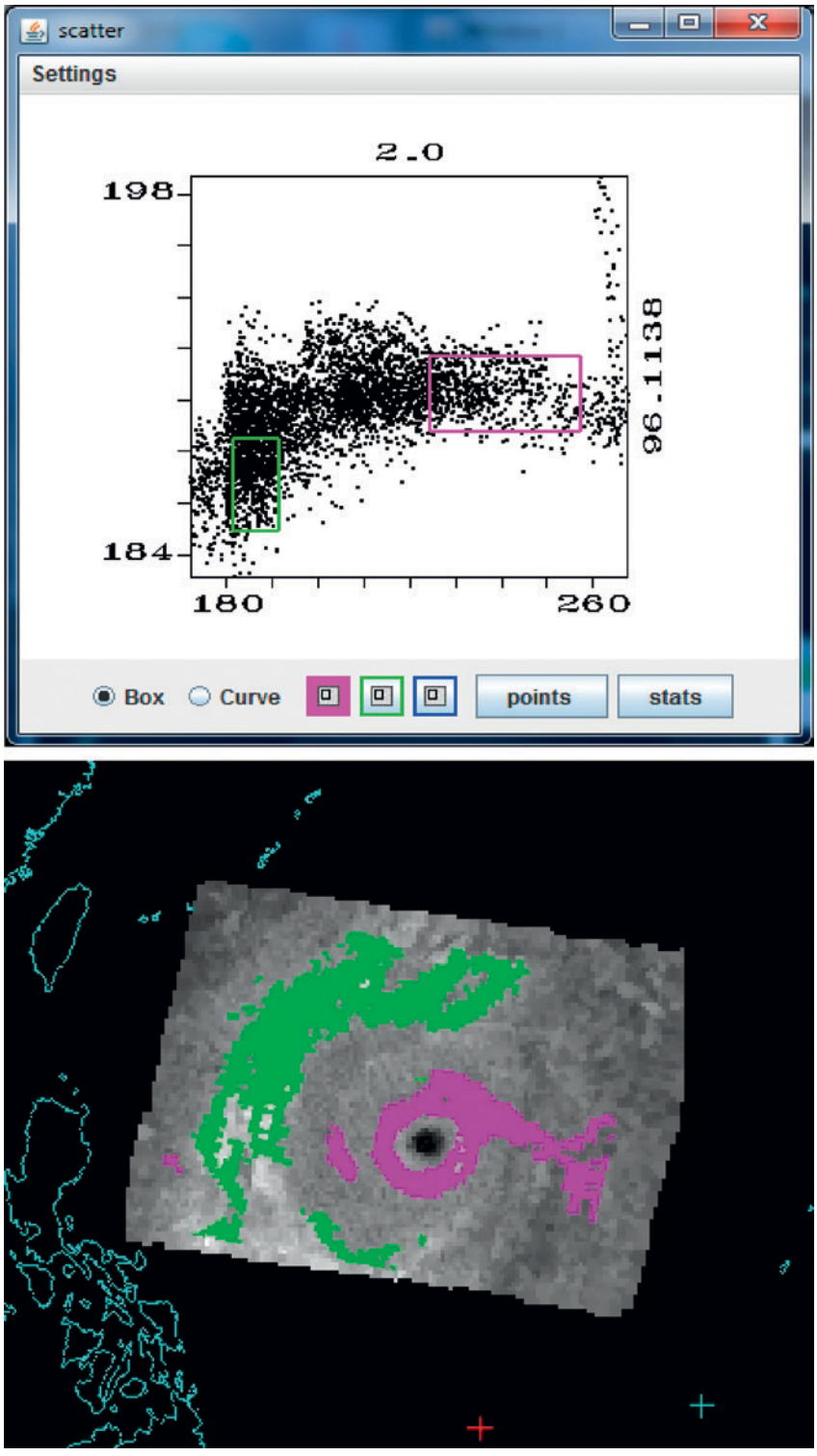

Fig. 12. (top) Scatterplot of ATMS 31.4-GHz (channel 2) brightness temperatures on the *x* axis vs dual-regression CrIS temperature retrievals at 96.1 hPa on the *y* axis. (bottom) Green and purple pixels from scatterplot located in the 96.1-hPa temperature image. All units are in kelvins.

Figure 12 shows a scatterplot of ATMS 31.4-GHz brightness temperatures (*x* axis) versus CrIS-derived temperatures retrieved for 96.1 hPa (*y* axis) over

Typhoon Vongfong. Different colored boxes highlight pixels in the scatterplot that are shown in the CrIS retrieval image; the cold ATMS temperatures reveal a ring of clouds in the northwest quadrant of Typhoon Vongfong, while the warm ATMS temperatures isolate the ring of clouds around the eye.

SUMMARY. HYDRA2 enables users from a variety of educational backgrounds to explore and investigate satellite sensor measurements. Starting from HYDRA, HYDRA2 has been adapted to accommodate data from more sensors, including those on *Suomi-NPP*. HYDRA2 has become a part of the Community Satellite Processing Package (CSPP), which can be found online (http://cimss.ssec.wisc.edu/cspp). The HYDRA2 command structure and enhanced visualizations tools are described in more detail online (http://cimss.ssec.wisc.edu/cspp/download/). Instructions for downloading this freeware are also provided on the website.

ACKNOWLEDGMENTS. This paper relied on extensive user participation that consisted of many students and international colleagues in beta testing the HYDRA2 freeware. We thank them for their enthusiasm and useful feedback. Funding from the NASA International MODIS/AIRS Processing Package (IMAPP) and the NOAA Community Satellite Processing Package (CSPP) programs is also gratefully acknowledged.

REFERENCES

Bill, R. W., 2002: *Jython for Java Programmers*. New Riders Publishing, 465 pp.

Hibbard, W., and Coauthors, 2002: Java distributed objects for numerical visualization in VisAD. *Commun. ACM*, **45**, 160–170, doi:10.1145/505248.506005.

Klaes, K. D., and Coauthors, 2007: An introduction to the EUMETSAT Polar System. *Bull. Amer. Meteor. Soc.*, **88**, 1085–1096, doi:10.1175/BAMS-88-7-1085.

Lutz, M., 1996: USENIX. *Programming Python: Object-Oriented Scripting*. O'Reilly Media, 902 pp.

Miller, S. D., S. P. Mills, C. D. Elvidge, D. T. Lindsey, T. F. Lee, and J. D. Hawkins, 2012: Suomi satellite brings to light a unique frontier of environmental imaging capabilities. *Proc. Natl. Acad. Sci. USA*, **109**, 15706–15711, doi:10.1073/pnas.1207034109.

Rink, T., P. Antonelli, T. Whittaker, K. Baggett, L. Gumley, A. Huang, and W. P. Menzel, 2007: Introducing HYDRA: A multispectral data analysis toolkit. *Bull. Amer. Meteor. Soc.*, **88**, 159–166, doi:10.1175/BAMS-88-2-159.

Weisz, E., W. L. Smith, and N. Smith, 2013: Advances in simultaneous atmospheric profile and cloud parameter regression based retrieval from high-spectral resolution radiance measurements. *J. Geophys. Res. Atmos.*, **118**, 6433–6443, doi:10.1002/jgrd.50521.